

The 3D $\pm J$ Ising model at the ferromagnetic transition line

Martin Hasenbusch,¹ Francesco Parisen Toldin,² Andrea Pelissetto,³ and Ettore Vicari¹

¹ *Dipartimento di Fisica dell'Università di Pisa and INFN, Pisa, Italy.*

² *Scuola Normale Superiore and INFN, Pisa, Italy.*

³ *Dipartimento di Fisica dell'Università di Roma "La Sapienza" and INFN, Roma, Italy.*

(Dated: November 1, 2018)

Abstract

We study the critical behavior of the three-dimensional $\pm J$ Ising model [with a random-exchange probability $P(J_{xy}) = p\delta(J_{xy}-J) + (1-p)\delta(J_{xy}+J)$] at the transition line between the paramagnetic and ferromagnetic phase, which extends from $p = 1$ to a multicritical (Nishimori) point at $p = p_N \approx 0.767$. By a finite-size scaling analysis of Monte Carlo simulations at various values of p in the region $p_N < p < 1$, we provide strong numerical evidence that the critical behavior along the ferromagnetic transition line belongs to the same universality class as the three-dimensional randomly-dilute Ising model. We obtain the results $\nu = 0.682(3)$ and $\eta = 0.036(2)$ for the critical exponents, which are consistent with the estimates $\nu = 0.683(2)$ and $\eta = 0.036(1)$ at the transition of randomly-dilute Ising models.

PACS numbers: 75.10.Nr, 75.40.Cx, 75.40.Mg, 64.60.Fr

I. INTRODUCTION

The $\pm J$ Ising model has played an important role in the study of the effects of quenched random disorder and frustration on Ising systems. It is defined by the lattice Hamiltonian

$$\mathcal{H}_{\pm J} = - \sum_{\langle xy \rangle} J_{xy} \sigma_x \sigma_y, \quad (1)$$

where $\sigma_x = \pm 1$, the sum is over the nearest-neighbor sites of a simple cubic lattice, and the exchange interactions J_{xy} are uncorrelated quenched random variables, taking values $\pm J$ with probability distribution

$$P(J_{xy}) = p\delta(J_{xy} - J) + (1 - p)\delta(J_{xy} + J). \quad (2)$$

For $p = 1$ we recover the standard Ising model, while for $p = 1/2$ we obtain the usual bimodal Ising spin-glass model.

The phase diagram of the three-dimensional (3D) $\pm J$ Ising model is sketched in Fig. 1. The high-temperature phase is paramagnetic for any p . The low-temperature phase depends on the value of p : it is ferromagnetic for small values of $1 - p$, while it is a spin-glass phase with vanishing magnetization for sufficiently large values of $1 - p$. The different phases are separated by transition lines, which meet at a multicritical point N located along the so-called Nishimori line.^{1,2,3} The spin-glass transition has been mostly studied at the symmetric point $p = 1/2$, see, e.g., Refs. 3,4 and references therein. The spin-glass transition line extends up to the Nishimori multicritical point,² located at^{5,6,7,8} $p_N \approx 0.767$. For larger values of p , the transition is ferromagnetic, up to $p = 1$ where one recovers the pure Ising model, and therefore a transition in the Ising universality class. At the ferromagnetic transition line, for $p_N < p < 1$, the critical behavior is expected to belong to a different universality class.

An interesting hypothesis, which has already been put forward in Refs. 3,9, is that the ferromagnetic transition of the $\pm J$ Ising model belongs to the 3D randomly-dilute Ising (RDIs) universality class (see, e.g., Refs. 10,11 for reviews on randomly-dilute spin models). A representative of the RDIs universality class is the randomly site-dilute Ising model (RSIM) defined by the lattice Hamiltonian

$$\mathcal{H}_d = -J \sum_{\langle xy \rangle} \rho_x \rho_y \sigma_x \sigma_y, \quad (3)$$

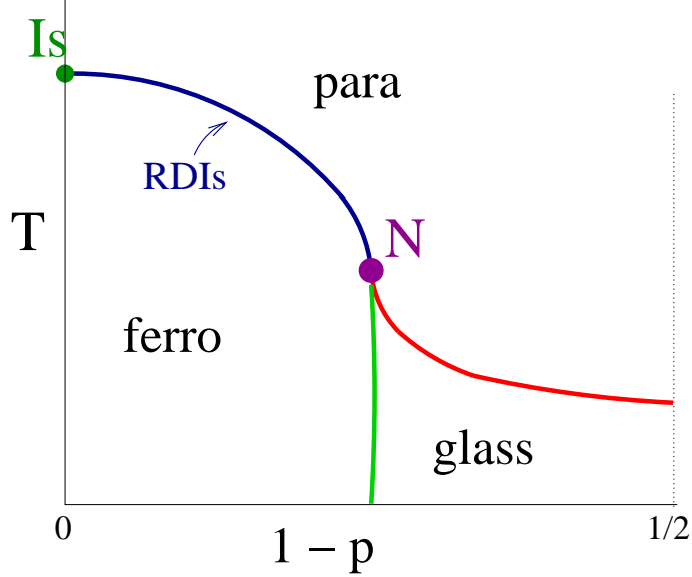


FIG. 1: Sketch of the phase diagram of the 3D $\pm J$ Ising model in the T - p plane.

where ρ_x are uncorrelated quenched random variables, which are equal to 0, 1 with probability

$$P(\rho_x) = p\delta(\rho_x - 1) + (1 - p)\delta(\rho_x). \quad (4)$$

For $p < 1$ and above the percolation threshold of the spins ($p_{\text{perc}} \approx 0.3116081(13)$ on a cubic lattice¹²), the RSIM undergoes a continuous phase transition between a disordered and a ferromagnetic phase, whose nature is independent of p . This transition is definitely different from the usual Ising transition: for instance, the correlation-length critical exponent^{13,14,15,16} $\nu = 0.683(2)$ differs from the Ising value^{17,18} $\nu = 0.63012(16)$. The RDIs universality class is expected to describe the ferromagnetic transition in generic diluted ferromagnetic systems. For instance, it has been verified that also the randomly bond-diluted Ising model (RBIM) belongs to the RDIs universality class.^{13,19} These results do not necessarily imply that also the $\pm J$ Ising model has an RDIs ferromagnetic transition line. Indeed, while the RSIM (3) has only ferromagnetic exchange interactions, the $\pm J$ Ising model is frustrated for any value of $p < 1$. Therefore, the ferromagnetic transition in the $\pm J$ Ising model belongs to the RDIs universality class only if frustration is irrelevant, a fact that is not obvious and should be carefully investigated.

Reference 9 investigated the issue by means of a Monte Carlo (MC) renormalization-group (RG) study, claiming that the $\pm J$ Ising model belongs to the same RDIs universality

class as the RSIM and the RBIM. It should be noted however that the quoted estimate for the correlation-length exponent at the ferromagnetic transition, $\nu = 0.658(9)$, is close to but not fully consistent with the RDIs value $\nu = 0.683(2)$.¹³ Another numerical MC work²⁰ investigated the nonequilibrium relaxation dynamics of the $\pm J$ Ising model and showed an apparent nonuniversal dynamical critical behavior along the ferromagnetic transition line. These results are not conclusive and further investigation is called for to clarify this issue.

In this paper we focus on the transition line of the 3D $\pm J$ Ising model between the paramagnetic and the ferromagnetic phase. We investigate the critical behavior by means of MC simulations at various values of p in the region $p_N < p < 1$. Our finite-size scaling (FSS) analysis provides a strong evidence that the critical behavior of the 3D $\pm J$ Ising along the ferromagnetic line belongs to the 3D RDIs universality class. For example, we obtain $\nu = 0.682(3)$ and $\eta = 0.036(2)$, which are in good agreement with the presently most accurate estimates¹³ $\nu = 0.683(2)$ and $\eta = 0.036(1)$ for the 3D RDIs universality class.

The paper is organized as follows. In Sec. II we summarize some FSS results which are needed for the analysis of the MC data, and describe our strategy to check whether the transition belongs to the RDIs universality class. In Sec. III we describe the MC simulations. In Sec. IV we report the results of the FSS analysis. Finally, in Sec. V we draw our conclusions. In App. A we report the definitions of the quantities we compute.

II. STRATEGY OF THE FINITE-SIZE SCALING ANALYSIS

In this work we check whether the ferromagnetic transition line in the 3D $\pm J$ Ising models belongs to the RDIs universality class. For this purpose, we present a FSS analysis of MC data for various values of p in the region $1 > p > p_N \approx 0.767$. We follow closely Ref. 13, which studied the ferromagnetic transition line in the 3D RSIM and RBIM and provided strong numerical evidence that these transitions belong to the same RDIs universality class. We refer to Ref. 13 for notations (a short summary is reported in App. A) and a detailed discussion of FSS in these disordered systems.

According to the RG, in the case of periodic boundary conditions and for $L \rightarrow \infty$, where L is the lattice size, a generic RG invariant quantity R at the critical temperature $1/\beta_c$ behaves as

$$R(L, \beta = \beta_c) = R^* \left(1 + c_{11}L^{-\omega} + c_{12}L^{-2\omega} + \dots + c_{21}L^{-\omega_2} + \dots \right), \quad (5)$$

where R^* is the universal infinite-volume limit and ω and ω_2 are the leading and next-to-leading correction-to-scaling exponents. In RDIs systems scaling corrections play an important role,^{16,21} since ω is quite small. Indeed we have $\omega = 0.33(3)$ and $\omega_2 = 0.82(8)$ in the 3D RDIs universality class.¹³ These slowly-decaying scaling corrections make the accurate determination of the universal asymptotic behavior quite difficult.

Instead of computing the various quantities at fixed Hamiltonian parameters, we keep a RG invariant quantity R fixed at a given value R_f .²² This means that, for each L , we determine the pseudocritical inverse temperature $\beta_f(L)$ such that

$$R(\beta = \beta_f(L), L) = R_f. \quad (6)$$

All interesting thermodynamic quantities are then computed at $\beta = \beta_f(L)$. The pseudocritical inverse temperature $\beta_f(L)$ converges to β_c as $L \rightarrow \infty$. The value R_f can be specified at will, as long as R_f is taken between the high- and low-temperature fixed-point values of R . The choice $R_f = R^*$ (where R^* is the critical-point value) improves the convergence of β_f to β_c for $L \rightarrow \infty$; indeed $\beta_f - \beta_c = O(L^{-1/\nu})$ for generic values of R_f , while $\beta_f - \beta_c = O(L^{-1/\nu-\omega})$ for $R_f = R^*$. This FSS method has already been applied to the study of the critical behavior of N -vector spin models,^{22,23} and of randomly-dilute Ising models.¹³

As in Ref. 13, we perform a FSS analysis at fixed $R_\xi \equiv \xi/L = 0.5943$, which is very close to the fixed-point value $R_\xi^* = 0.5944(7)$ of R_ξ at β_c . Given any RG invariant quantity R , such as the quartic cumulants U_4 and U_{22} , we consider its value at fixed R_ξ , i.e., $\bar{R}(L) = R(L, \beta_f(L))$. For $L \rightarrow \infty$, $\bar{R}(L)$ behaves as $R(L, \beta_c)$:

$$\bar{R}(L) = \bar{R}^* (1 + b_{11}L^{-\omega} + b_{12}L^{-2\omega} + \dots + b_{21}L^{-\omega_2} + \dots), \quad (7)$$

where the coefficients b_{ij} depend on the Hamiltonian. The derivative \bar{R}' with respect to β of a generic RG invariant quantity R behaves as

$$\bar{R}'(L) = aL^{1/\nu} (1 + a_{11}L^{-\omega} + a_{12}L^{-2\omega} + \dots + a_{21}L^{-\omega_2} + \dots). \quad (8)$$

Finally, the FSS of the magnetic susceptibility χ is given by¹³

$$\bar{\chi}(L) \equiv \chi(L, \beta = \beta_f(L)) = eL^{2-\eta} (1 + e_{11}L^{-\omega} + e_{12}L^{-2\omega} + \dots + e_{21}L^{-\omega_2} + \dots) + e_b \quad (9)$$

where e_b represents the background contribution.

A standard RG analysis, see, e.g., Ref. 13, shows that the amplitudes of the $O(L^{-k\omega})$ scaling corrections are proportional to u_3^k (with a universal coefficient), where u_3 is the

leading irrelevant scaling field with RG dimension $y_3 = -\omega$. Hamiltonians such that $u_3 = 0$ —we call them *improved* Hamiltonians—have a faster approach to the universal asymptotic behavior, because the $O(L^{-k\omega})$ scaling corrections vanish: $b_{1k} = a_{1k} = e_{1k} = 0$ in Eqs. (7), (8), and (9). In this case the leading scaling corrections are proportional to $u_4 L^{-\omega_2}$, where u_4 is the next-to-leading irrelevant scaling field and $y_4 = -\omega_2$ is its RG dimension. In Ref. 13 it was shown that the RSIM for $p = p^* = 0.800(5)$ and the RBIM for $p = p^* = 0.56(2)$ are improved. Since scaling fields are analytic functions of the Hamiltonian parameters, u_3 must be proportional to $p - p^*$ close to $p = p^*$, i.e. $u_3 \approx c_3(p - p^*)$. Therefore, since the coefficients b_{1k} , a_{1k} , and e_{1k} that appear in Eqs. (7), (8), and (9) are proportional to u_3^k , we have

$$b_{1k}, a_{1k}, e_{1k} \sim (p - p^*)^k. \quad (10)$$

Beside the quantities defined in App. A, we also consider observables—in analogy with the previous terminology, we call them improved quantities—characterized by the fact that the leading scaling correction proportional to $L^{-\omega}$ (approximately) vanishes in any model belonging to the RDIs universality class.¹³ We consider the combination of quartic cumulants

$$\bar{U}_{\text{im}} = \bar{U}_4 + 1.3\bar{U}_{22}, \quad (11)$$

and improved estimators of the critical exponent ν defined as

$$R'_{\xi, \text{im}} \equiv \bar{R}'_{\xi} \bar{U}_d^4, \quad U'_{4, \text{im}} \equiv \bar{U}'_4 \bar{U}_d^{2.5} \quad (12)$$

(\bar{U}_d is defined in App. A). In Ref. 13 we showed that, if the transition belongs to the RDIs universality class, the leading scaling correction proportional to $L^{-\omega}$ of these improved observables is suppressed. More precisely, we showed that the universal ratio of the amplitudes of the leading scaling correction in \bar{U}_{im} and \bar{U}_4 satisfies

$$|b_{11, \bar{U}_{\text{im}}}/b_{11, \bar{U}_4}| \lesssim \frac{1}{15}, \quad (13)$$

while the one for the quantities $R'_{\xi, \text{im}}$ and \bar{R}'_{ξ} is bounded by

$$|a_{11, R'_{\xi, \text{im}}}/a_{11, \bar{R}'_{\xi}}| \lesssim \frac{1}{4}. \quad (14)$$

The remaining scaling corrections are of order $L^{-2\omega}$ and $L^{-\omega_2}$. These improved observables are particular useful to check whether the transition in a given system belongs to the 3D RDIs universality class.

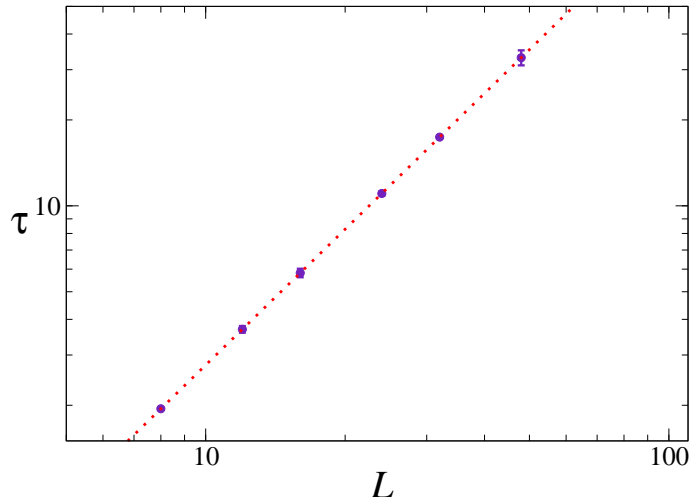


FIG. 2: Exponential autocorrelation time τ of the magnetic susceptibility for a mixture of Metropolis and cluster updates as discussed in the text, at $p = 0.87$. The dotted line shows the result of a fit to $\tau = cL^z$: this fit gives $z \approx 1.6$.

To summarize: in order to check whether the ferromagnetic transition of the 3D $\pm J$ Ising model belongs to the RDIs universality class, we perform a FSS analysis at fixed $R_\xi = 0.5943$, and check if the results for the critical exponents and other universal quantities are consistent with those obtained for the RDIs universality class, which is characterized by¹³ critical exponents $\nu = 0.683(2)$ and $\eta = 0.036(1)$, by the leading and next-to-leading scaling-correction exponents $\omega = 0.33(3)$ and $\omega_2 = 0.82(8)$ and by the universal infinite-volume values of the quartic cumulants $\bar{U}_{22}^* = 0.148(1)$, $\bar{U}_{\text{im}}^* = 1.840(4)$, and $\bar{U}_d^* = 1.500(1)$. Notice that the fact that we fix $R_\xi = 0.5943$ does not introduce any bias in our FSS analysis.

III. MONTE CARLO SIMULATIONS

We performed MC simulations of Hamiltonian (1) with $J = 1$ for $p = 0.94, 0.90, 0.883, 0.87, 0.83, 0.80$, close to the critical temperature on cubic lattices of size L^3 with periodic boundary conditions, for a large range of lattice sizes: from $L = 8$ to $L = 80$ for $p = 0.883, 0.87$, to $L = 64$ for $p = 0.94, 0.90, 0.83$, and to $L = 48$ for $p = 0.80$. We chose values of p not too close to $p = 1$: indeed, as $p \rightarrow 1$ we expect crossover effects due to the presence of the Ising transition for $p = 1$ and, therefore, that the asymptotic behavior sets in only for large values of L . We return to this point later.

We used a Metropolis algorithm and multispin coding.²⁴ In the simulation n_{bit} systems evolve in parallel, where $n_{\text{bit}} = 32$ or $n_{\text{bit}} = 64$ depending on the computer that is used. For each of these n_{bit} systems we use a different set of couplings J_{xy} . This allows us to perform 64 parallel simulations on a 64-bit machine, and therefore to gain a large factor in the efficiency of the MC simulations. We used high-quality random-number generators, such as the RANLUX²⁵ or the twister²⁶ generators.²⁷ Using the twister random-number generator, we need about 1.2×10^{-9} seconds for one Metropolis update of a single spin on an Opteron processor running at 2 GHz. Our simulations took approximately 3 CPU years on an Opteron (2 GHz) processor.

It is worth mentioning that cluster algorithms, such as the Swendsen-Wang cluster²⁸ and the Wolff single-cluster²⁹ algorithm, show significant slowing down in the $\pm J$ Ising model. At the earlier stage of this work we performed some simulations of the $\pm J$ Ising model at $p = 0.87$ using the algorithm used in Ref. 13 to simulate the RSIM and the RBIM. There we used a combination of Metropolis, Swendsen-Wang cluster,²⁸ and Wolff single-cluster²⁹ updates. More precisely, each updating step consisted of 1 Swendsen-Wang update, 1 Metropolis update, and L single-cluster updates. In all cases the exponential autocorrelation times τ of the magnetic susceptibility was small: $\tau \lesssim 1$ in units of the above updating step, even for the largest lattice sizes considered, i.e. $L = 192$. In the $\pm J$ Ising model at $p = 0.87$ autocorrelation times are much larger. In Fig. 2 we plot estimates of τ as obtained from the magnetic susceptibility. They show a clear evidence of critical slowing down: $\tau \sim L^z$ with $z \approx 1.6$. Such a value of z should be compared with the dynamic exponent of Swendsen-Wang and Wolff cluster algorithms in the RSIM, which is much smaller:³⁰ $z \lesssim 0.5$. These results show that cluster algorithms behave differently in the $\pm J$ Ising model, likely due to frustration. They suggest that frustration is relevant for the cluster dynamics.

Taking also into account the computer time required by the cluster algorithms, we then turned to a multispin Metropolis algorithm. This turns out to be much more effective at the lattice sizes considered, although it has a larger dynamic exponent $z \gtrsim 2$, see, e.g., Ref. 30 and references therein. We also mention that the autocorrelation time significantly increases with decreasing p (keeping L fixed). For example, for $L = 48$ it increases by approximately a factor of 10 from $p = 0.90$ to $p = 0.80$. This represents a major limitation to perform simulations for large lattices close to the multicritical point.

For each lattice size we considered N_s disorder samples, with N_s decreasing with increasing L , from $N_s \gtrsim 10^6$ for $L = 8$ to $N_s \gtrsim 2 \times 10^4$ for the largest lattices. For each disorder sample, we collected a few hundred independent measurements at equilibrium. The averages over disorder are affected by a bias due to the finite number of measures at fixed disorder.^{13,31} A bias correction is required whenever one considers the disorder average of combinations of thermal averages. We used the formulas reported in App. B of Ref. 13. Errors were computed from the sample-to-sample fluctuations and were determined by using the jackknife method.²⁷

Our FSS analysis is performed at fixed $R_\xi \equiv \xi/L$. In order to determine expectation values at fixed R_ξ , one needs the values of the observables as a function of β in some neighborhood of the inverse temperature β_{run} used in the simulation. In Ref. 13 we used the reweighting method for this purpose. This requires that the observables and, in particular, the values of the energy are stored at each measurement. For the huge statistics like those we have for the smaller values of L , this becomes unpractical. Therefore, we used here a second-order Taylor expansion, determining $O(\beta, L)$ from $O(\beta_{\text{run}}, L) + a_O(\beta - \beta_{\text{run}}) + b_O(\beta - \beta_{\text{run}})^2$. The coefficients a_O and b_O are obtained from appropriate expectation values as in Ref. 23. Since their computation involves disorder averages of products of thermal averages, we have implemented in all cases an exact bias correction, using the formulas of Ref. 13. Derivatives with respect to β are then obtained as $O'(\beta, L) = a_O + 2b_O(\beta - \beta_{\text{run}})$. Of course, this method requires $|\beta_{\text{run}} - \beta_f|$ to be sufficiently small. We have carefully checked the results by performing, for each L and p , runs at different values of β .

The MC estimates of the quantities introduced in Sec. II and in App. A at fixed $R_\xi \equiv \xi/L = 0.5943$ are available on request.

IV. FINITE-SIZE SCALING ANALYSIS

In this section we present the results of our FSS analysis of the MC data at fixed $R_\xi = 0.5943$.

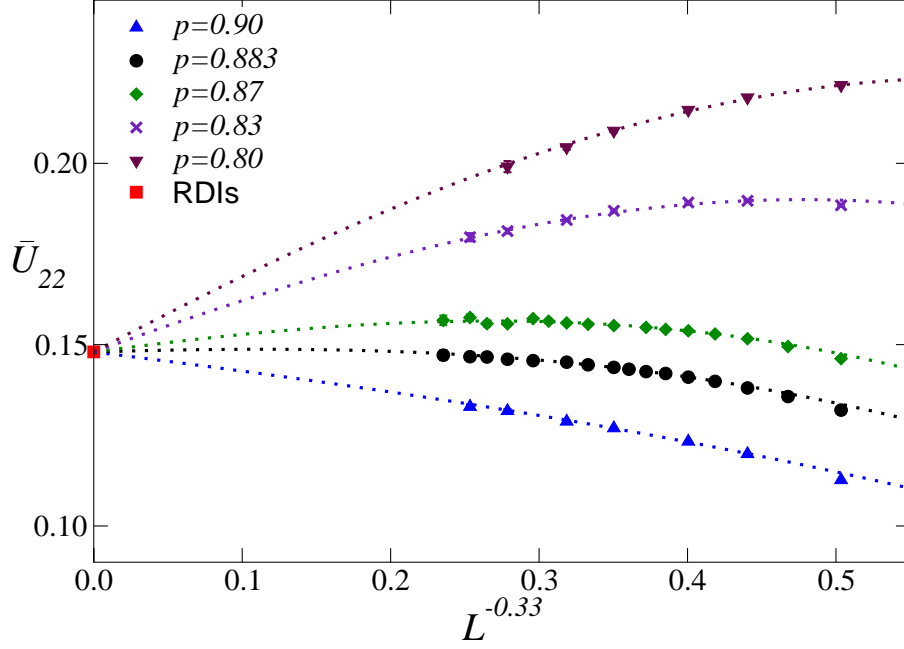


FIG. 3: MC estimates of \bar{U}_{22} versus $L^{-\omega}$ with $\omega = 0.33$ for different values of p . The dotted lines show results of fits to $c_0 + c_1 L^{-\varepsilon_1} + c_2 L^{-\varepsilon_2}$, fixing $c_0 = 0.148$, $\varepsilon_1 = 0.33$, and $\varepsilon_2 = 0.82$. In the RDIs universality class $\bar{U}_{22}^* = 0.148(1)$.¹³

A. Renormalization-group invariant quantities

In Fig. 3 we show the MC estimates of \bar{U}_{22} versus $L^{-\omega}$ with $\omega = 0.33(3)$, which is the leading scaling exponent of the RDIs universality class. The data vary significantly with p and L . This p and L dependence is always consistent with the existence of the expected next-to-leading scaling corrections, i.e. with a behavior of the form

$$\bar{U}_{22} = \bar{U}_{22}^* + c_1 L^{-\varepsilon_1} + c_2 L^{-\varepsilon_2}, \quad (15)$$

where \bar{U}_{22}^* , ε_1 and ε_2 are fixed to the RDIs values:¹³ $\bar{U}_{22}^* = 0.148$, $\varepsilon_1 = 0.33$ and $\varepsilon_2 = 0.66, 0.82$. The fits corresponding to $\varepsilon_2 = 0.82$ are shown in Fig. 3. Note that in most of the cases it is crucial to include a next-to-leading correction. Only for $p = 0.90$ the data are well fitted by taking only the leading scaling correction.

An unbiased estimate of ω can be obtained from the difference of data at different values of p , i.e. by considering

$$\bar{U}_{22}(p_1; L) - \bar{U}_{22}(p_2; L) \approx cL^{-\omega}. \quad (16)$$

Linear fits of the logarithm of these differences give results in reasonable agreement with

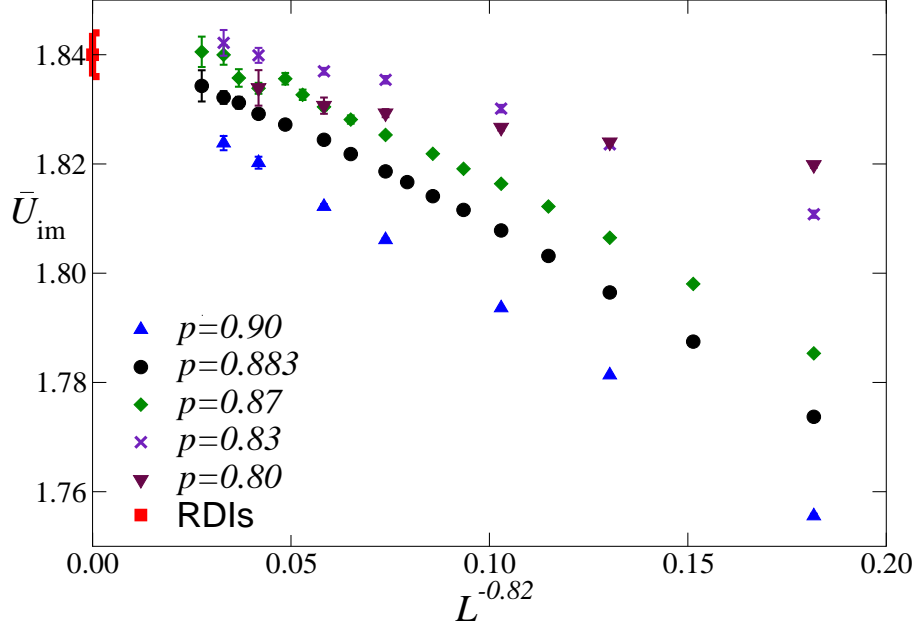


FIG. 4: MC estimates of \bar{U}_{im} versus $L^{-0.82}$. The filled square on the vertical axis corresponds to the RDIs estimate¹³ $\bar{U}_{\text{im}}^* = 1.840(4)$.

the RDIs estimate $\omega = 0.33(3)$, especially when only data corresponding to $L \geq L_{\text{min}} = 24$ are used. For $L_{\text{min}} = 24$ [$L_{\text{min}} = 32$], we obtain $\omega = 0.27(2)$ [$\omega = 0.27(3)$] from the data at $p_1 = 0.83$ and $p_2 = 0.90$, $\omega = 0.19(5)$ [$\omega = 0.31(9)$] from those at $p_1 = 0.883$ and $p_2 = 0.90$, and $\omega = 0.29(3)$ [$\omega = 0.25(4)$] from the results at $p_1 = 0.83$ and $p_2 = 0.883$. We also fitted the difference $\bar{U}_{22} - 0.148$ at $p = 0.90$ to $cL^{-\varepsilon}$ (for this value of p next-to-leading corrections are apparently very small, see Fig. 3). We obtain $\omega = 0.35(3)$ [$\omega = 0.39(6)$] for $L_{\text{min}} = 24$ [$L_{\text{min}} = 32$].

The results of the above-reported fits of \bar{U}_{22} show that the leading scaling corrections proportional to $L^{-\omega}$ vanish for $p \approx 0.883$. Note that, close to p^* , the relevant next-to-leading scaling corrections should be those proportional to $L^{-\omega_2}$ with $\omega_2 \approx 0.82$. Indeed, according to Eq. (10), the coefficient of those proportional to $L^{-2\omega}$ is of order $(p - p^*)^2$, i.e. $b_{12} \approx \bar{b}_{12}(p - p^*)$. Therefore, b_{12} is small if $\bar{b}_{12} = O(1)$ (we checked this numerically). This applies to the FSS at $p = 0.87$ and 0.90 , where the $L^{-2\omega}$ corrections can be neglected, although in these two cases we cannot neglect the leading $L^{-\omega}$ correction whose coefficient is proportional to $p - p^*$. An analysis of the leading scaling corrections at $p = 0.87, 0.883, 0.90$, assuming the RDIs values $\bar{U}_{22}^* = 0.148(1)$ and $\omega = 0.33(3)$ (we perform combined fits to (15)

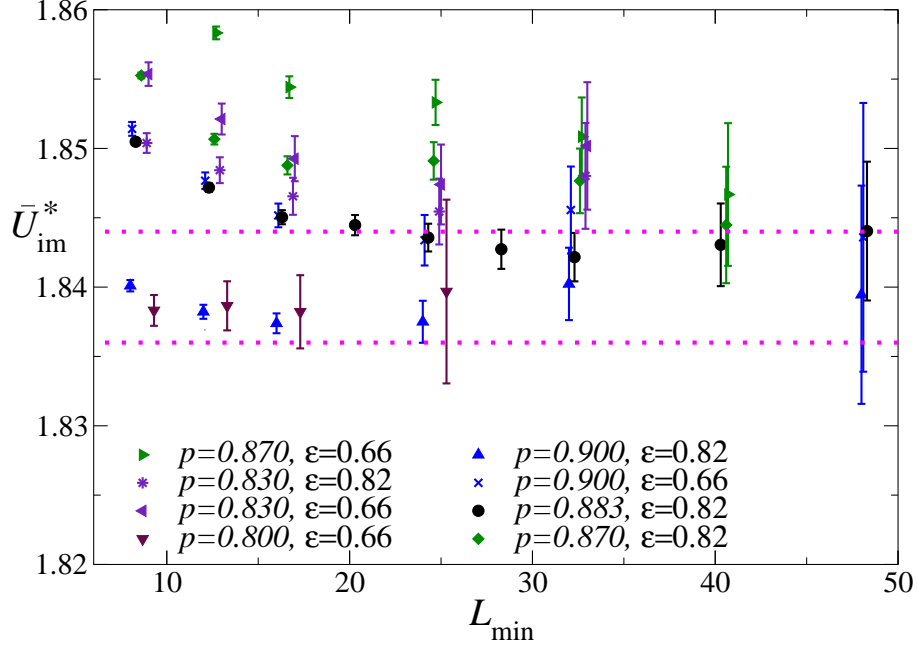


FIG. 5: Estimates of \bar{U}_{im}^* as obtained by fits to $\bar{U}_{\text{im}}^* + cL^{-\epsilon}$, versus the minimum lattice size L_{min} allowed in the fits. Some data are slightly shifted along the x -axis to make them visible. The dotted lines correspond to the RDIs estimate¹³ $\bar{U}_{\text{im}}^* = 1.840(4)$.

with $\epsilon_1 = \omega$) gives the estimate

$$p^* = 0.883(3), \quad (17)$$

which is approximately in the middle of the ferromagnetic line, i.e. $1 - p^* \approx (1 - p_N)/2$. We performed a similar analysis for \bar{U}_d , obtaining a consistent estimate of p^* . Thus, the $\pm J$ Ising model for $p = 0.883$ is approximately improved. Therefore, at $p = 0.883$, fits of the data assuming $O(L^{-\omega_2})$ leading scaling corrections should provide reliable results.

As discussed in Sec. II, a useful quantity to perform stringent checks of universality within the RDIs universality class is the combination \bar{U}_{im} of quartic cumulants reported in Eq. (11). For this quantity the scaling corrections proportional to $L^{-\omega}$ are small, cf. Eq. (13), and thus the dominant corrections should behave as $L^{-2\omega}$, with $2\omega \approx 0.66$. As already discussed, for values of p close to p^* , such as $p = 0.87, 0.883, 0.90$, also the $L^{-2\omega}$ term is expected to be small and thus the dominant corrections should scale as $L^{-\omega_2}$ with $\omega_2 \approx 0.82$. In Fig. 4 we show the MC results for \bar{U}_{im} for various values of p . Fig. 5 shows results of fits to

$$\bar{U}^* + cL^{-\epsilon}, \quad (18)$$

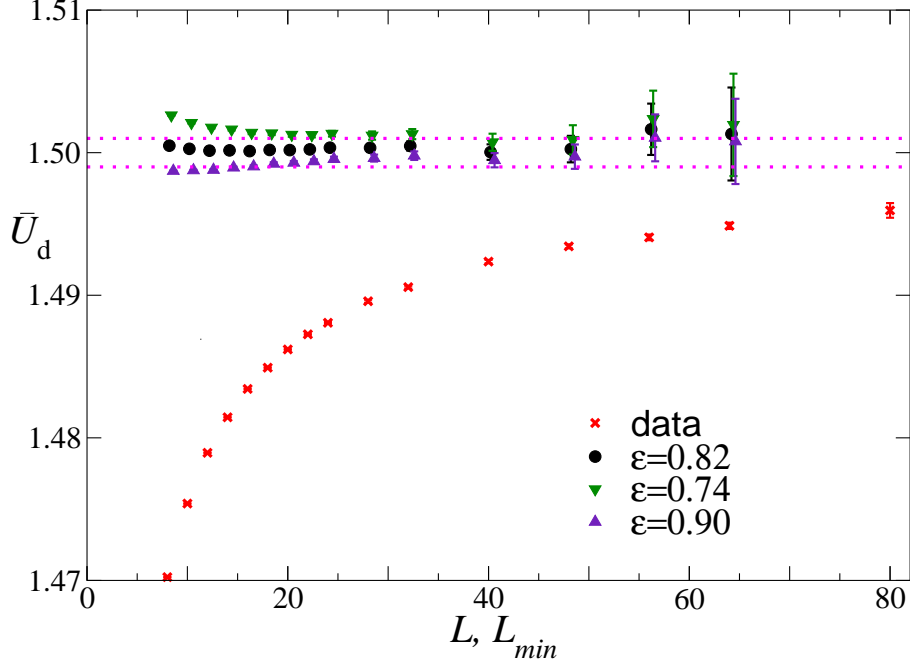


FIG. 6: Estimates of \bar{U}_d^* as obtained by fits of \bar{U}_d at $p = 0.883$, to $\bar{U}_d^* + cL^{-\varepsilon}$. Some data are slightly shifted along the x -axis to make them visible. The dotted lines correspond to the RDIs estimate¹³ $\bar{U}_d^* = 1.500(1)$.

with $\varepsilon = 0.66, 0.82$. We obtain $\bar{U}_{\text{im}}^* = 1.840(3)[3], 1.842(2)[1], 1.845(2)[3]$ respectively for $p = 0.90, 0.883, 0.87$, fixing $\varepsilon = \omega_2 = 0.82(8)$ (the error in brackets is related to the uncertainty of ω_2) and using data with $L \geq 32$; moreover we obtain $\bar{U}_{\text{im}}^* = 1.847(3)[2], 1.840(7)[1]$ respectively for $p = 0.83, 0.80$, fixing $\varepsilon = 0.66(6)$ and using data with $L \geq 24$. For all values of p the results are in good agreement with RDIs estimate¹³ $\bar{U}_{\text{im}}^* = 1.840(4)$. They provide strong support to a RDIs critical behavior along the ferromagnetic line.

A further stringent check of universality comes from the analysis of the data \bar{U}_d at $p = 0.883$, because the data of \bar{U}_d are very precise due to a cancellation of the statistical fluctuations.¹³ Since the model is improved, the $L^{-k\omega}$ scaling corrections are negligible and the large- L behavior is approached with corrections of order $L^{-\omega_2}$, $\omega_2 = 0.82(8)$. We thus fit the data to Eq. (18) with $\varepsilon = 0.74, 0.82, 0.90$. In Fig. 6 we show the results. We obtain $\bar{U}_d^* = 1.5001(1)[15], 1.5004(2)[9], 1.5003(10)[6]$ (the error in brackets is related to the uncertainty of $\omega_2 = 0.82(8)$) for $L_{\text{min}} = 12, 24, 48$ respectively. Moreover, by fitting the data to $\bar{U}_d^* + c_1L^{-\varepsilon_1} + c_2L^{-\varepsilon_2}$ with $\varepsilon_1 = 0.33$ and $\varepsilon_2 = 0.82$, we obtain $\bar{U}_d^* = 1.5006(7), 1.500(3)$ for $L_{\text{min}} = 12, 24$ respectively. These results are in perfect agreement with the RDIs estimate¹³

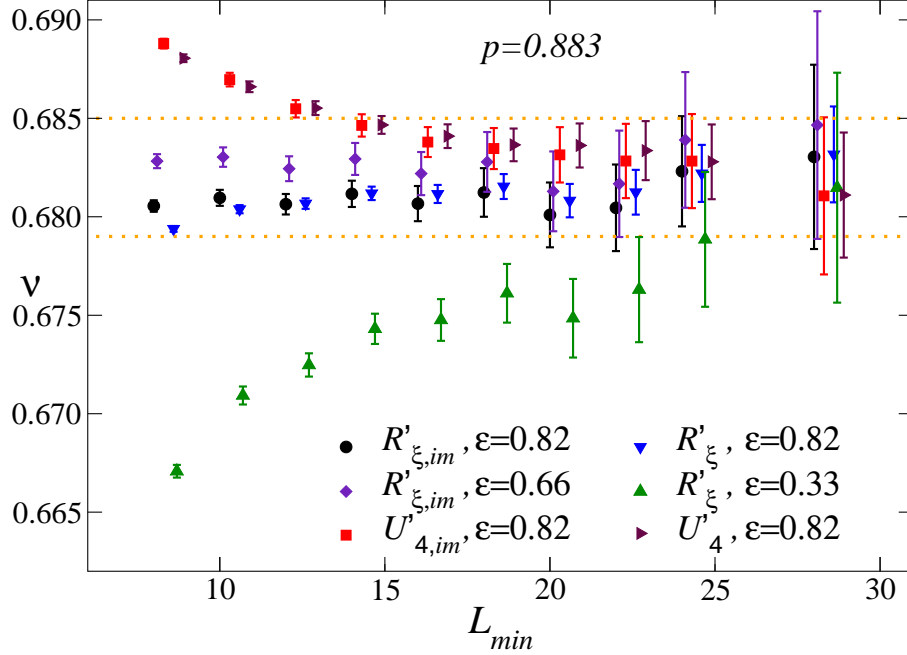


FIG. 7: Estimates of the critical exponent ν , as obtained by fits of \bar{R}'_{ξ} , \bar{U}'_4 , $R'_{\xi,im}$, and $U'_{4,im}$ at $p = 0.883$. L_{min} is the minimum lattice size allowed in the fits. Some data are slightly shifted along the x -axis to make them visible. The dotted lines correspond to the estimate $\nu = 0.682(3)$.

$\bar{U}_d^* = 1.500(1)$. Such an agreement is also confirmed by the analysis of the data of \bar{U}_{22} , for example a fit to Eq. (18) with $\varepsilon = \omega_2 = 0.82(8)$ gives $\bar{U}_{22}^* = 0.1486(8)[3]$ for $L_{min} = 32$, to be compared with the RDIs estimate¹³ $\bar{U}_{22}^* = 0.148(1)$.

We have not shown results for values of p too close to 1, for $p > 0.90$ say, because they are affected by crossover effects due to presence of the Ising transition for $p = 1$, as it also occurs in randomly dilute Ising models.^{16,21,32} For instance, for $p = 0.94$ the data are not compatible with a behavior of the form (15) with \bar{U}_{22}^* fixed to the RDIs value. Our data that correspond to lattice sizes $L \leq 64$ apparently converge to a smaller value, consistently with the expected crossover from pure to random behavior (in pure systems $\bar{U}_{22}^* = 0$). The same quantitative differences are observed in the RSIM and in the RBIM close to the Ising transition. This suggests that in FSS analyses up to $L \approx 100$ the asymptotic RDIs behavior can only be observed for $p \lesssim 0.94$.

B. Critical exponents

The correlation-length exponent ν can be estimated by fitting the derivative of R_ξ and U_4 to the expression (8). Accurate estimates are only obtained for improved Hamiltonians. For generic models, as shown in Ref. 13, good estimates are only obtained by using improved estimators, such as those reported in Eq. (12).

We analyze the data at $p = 0.883$, which is a very good approximation of the improved value $p^* = 0.883(3)$. In Fig. 7 we report several results for the critical exponent ν , obtained by analyzing \bar{R}'_ξ , \bar{U}'_4 , and their improved versions $R'_{\xi,\text{im}}$ and $U'_{4,\text{im}}$. We show results of fits of their logarithms to

$$\frac{1}{\nu} \ln L + a + bL^{-\varepsilon}, \quad (19)$$

fixing ε to several values. Since the Hamiltonian is approximately improved, scaling corrections are expected to decrease as $L^{-\omega_2}$ with $\omega_2 = 0.82(8)$. Since $p = 0.883$ is only approximately equal to p^* , one may be worried of the residual leading scaling corrections that are small but do not vanish exactly. Improved estimators should provide the most reliable results since the leading scaling corrections are additionally suppressed.

As can be seen in Fig. 7, the results obtained by using \bar{R}'_ξ and \bar{U}'_4 and $\varepsilon = 0.82$ are perfectly consistent with those obtained from their improved versions. This confirms that the Hamiltonian is improved. Fits of \bar{R}'_ξ to (19) with $\varepsilon = 0.33$ do not provide stable results. The results approach the values obtained in the other fits only when increasing the minimum size L_{min} allowed in the fit. This is expected, since the $L^{-\omega}$ corrections should be negligible with respect to the $L^{-\omega_2}$ ones. In conclusion, our final estimate of the correlation-length exponent is

$$\nu = 0.682(3), \quad (20)$$

which includes all results (with their errors) of the fits of \bar{R}'_ξ , \bar{U}'_4 , $R'_{\xi,\text{im}}$, $U'_{4,\text{im}}$ to Eq. (19) with $\varepsilon = 0.82(8)$ and $L_{\text{min}} = 16, 24$. Estimate (20) is in perfect agreement with the most precise RDIs estimate $\nu = 0.683(2)$.

Estimate (20) is also confirmed by the analysis of the data at the other values of p . Fig. 8 shows results obtained by fitting the logarithm of $R'_{\xi,\text{im}}$ to the function (19) for other values of p . They are definitely consistent with the result obtained at $p = 0.883$. Results for $p = 0.80$ are not shown because the available data are not sufficient to get reliable results.

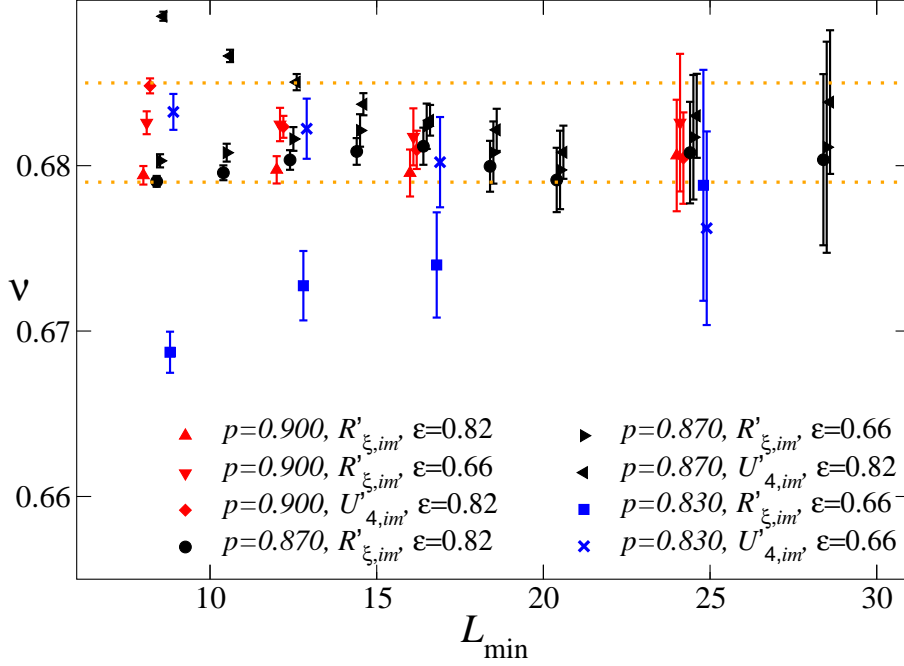


FIG. 8: Results from ν obtained by fitting $R'_{\xi,im'}$ to $aL^{1/\nu}(1+bL^{-\epsilon})$. Some data are slightly shifted along the x -axis to make them visible. The dotted lines correspond to the estimate obtained at $p = 0.883$, i.e. $\nu = 0.682(3)$.

In order to estimate the critical exponent η , we analyze the FSS of the magnetic susceptibility $\bar{\chi}$, cf. Eq. (9). We fit it to $aL^{2-\eta} + b$ (where b represents a constant background term), to $aL^{2-\eta}(1 + cL^{-\epsilon})$, and to $aL^{2-\eta}(1 + cL^{-\epsilon}) + b$ (more precisely, we fit $\ln \bar{\chi}$ to the logarithm of the previous expressions). The results at $p = 0.883$ are shown in Fig. 9, versus the minimum size L_{\min} allowed in the fits. We obtain the estimate

$$\eta = 0.036(2), \quad (21)$$

which includes all results obtained for $L_{\min} \gtrsim 16$. This estimate agrees with the most precise RDIs estimate $\eta = 0.036(1)$. Fig. 10 shows results for the other values of p . Again, they are in good agreement.

C. The critical temperature

The critical temperature can be estimated by extrapolating the estimates of β_f at $R_\xi = 0.5943$, cf. Eq. (6). Since we have chosen $R_\xi = 0.5943 \approx R_\xi^* = 0.5944(7)$,¹³ we expect

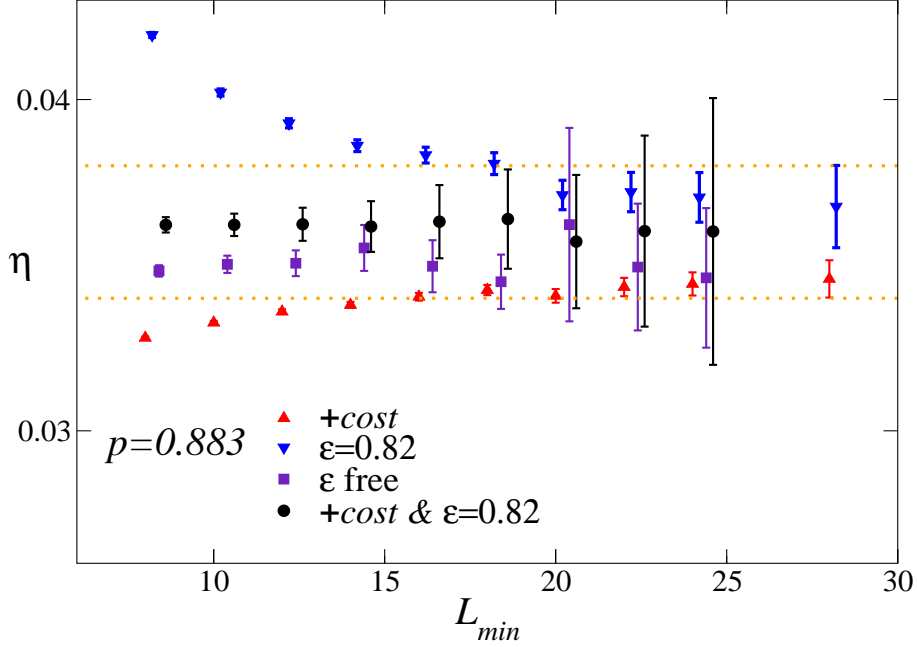


FIG. 9: Estimates of the critical exponent η , obtained by fitting $\ln \bar{\chi}$ at $p = 0.883$, to $a + (2 - \eta) \ln L + bL^{\eta-2}$ (denoted by *+cost*), $a + (2 - \eta) \ln L + a_1 L^{-\varepsilon}$, and to $a + (2 - \eta) \ln L + a_1 L^{-\varepsilon} + bL^{\eta-2}$. Some data are slightly shifted along the x -axis to make them visible. The dotted lines correspond to the final estimate $\eta = 0.036(2)$.

in general that $\beta_f - \beta_c = O(L^{-1/\nu-\omega})$. For $p = 0.883$, since the model is approximately improved, the leading scaling corrections are related to the next-to-leading exponent ω_2 . Thus, in this case $\beta_f - \beta_c = O(L^{-1/\nu-\omega_2})$. This behavior is nicely observed in Fig. 11, which shows $\beta_f(L)$ at $p = 0.883$ vs $L^{-1/\nu-\omega_2}$ with $1/\nu + \omega_2 \approx 2.28$. A fit to $\beta_c + aL^{-1/\nu-\omega_2}$ gives $\beta_c = 0.300611(1)$.

For the other values of p we expect $\beta_f - \beta_c = O(L^{-1/\nu-\omega})$ with $1/\nu + \omega \approx 1.79$. Linear fits of $\beta_f(L)$ (for $L \geq L_{\min}$ with L_{\min} sufficiently large to give an acceptable χ^2) give the estimates $\beta_c = 0.25544(2)$ for $p = 0.94$, $\beta_c = 0.285285(5)$ for $p = 0.90$, $\beta_c = 0.313748(1)$ for $p = 0.87$, $\beta_c = 0.365459(5)$ for $p = 0.83$, $\beta_c = 0.42501(3)$ for $p = 0.80$. We finally recall that¹⁸ $\beta_c = 0.22165452(8)$ for $p = 1$ (the standard Ising model), and that⁷ $\beta_c = 0.5967(11)$ at the multicritical Nishimori point at $p_N = 0.7673(3)$. In Fig. 12 we plot the available estimates of the critical temperature $T_c \equiv 1/\beta_c$ in the region $1 \geq p \geq p_N$.

The estimates of T_c shown in Fig. 12 hint at a smooth linear behavior for small values of $w \equiv 1 - p$, close to the Ising point at $w = 0$. This can be explained by some considerations

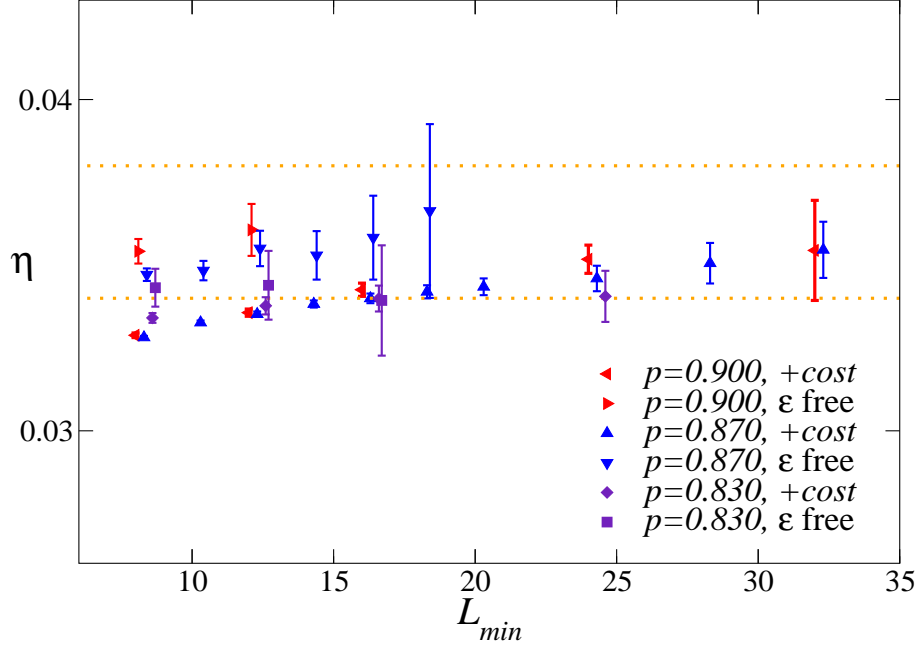


FIG. 10: Estimates of the critical exponent η , obtained by fitting $\bar{\chi}$ for various values of p . See the caption of Fig. 9 for an explanation of the fits. Some data are slightly shifted along the x -axis to make them visible. The dotted lines correspond to the result $\eta = 0.036(2)$ obtained at $p = 0.883$.

on the multicritical behavior around the Ising point at $w = 0$. The Ising critical behavior at $w = 0$ is unstable against the RG perturbation induced by quenched disorder at $w > 0$,³³ which leads to the RDIs critical behavior. Indeed such a perturbation has a positive RG dimension y_w at the Ising fixed point:^{10,34} $y_w = \alpha_{\text{Is}}/\nu_{\text{Is}} = 2/\nu_{\text{Is}} - 3$ where α_{Is} and ν_{Is} are the Ising specific-heat and correlation-length critical exponents, and therefore¹⁷ $y_w = 0.1740(8)$. Thus, in the absence of an external magnetic field, beside the scaling field u_t related to the temperature, there is another relevant scaling field u_w associated with the quenched disorder parameter $w \equiv 1 - p$. General RG scaling arguments^{21,35} show that the singular part of the free energy for $w \rightarrow 0$ behaves as

$$\mathcal{F}_{\text{sing}} \sim u_t^{2-\alpha_{\text{Is}}} F(X), \quad X = u_w u_t^{-\phi}, \quad (22)$$

where $\phi = y_w \nu_{\text{Is}} = \alpha_{\text{Is}} = 0.1096(5)$ is the crossover exponent, and $F(X)$ is a crossover scaling function which is universal (apart from normalizations). The scaling fields u_t and u_w depend on the parameters of the model. In general, we expect

$$u_t = t + kw, \quad (23)$$

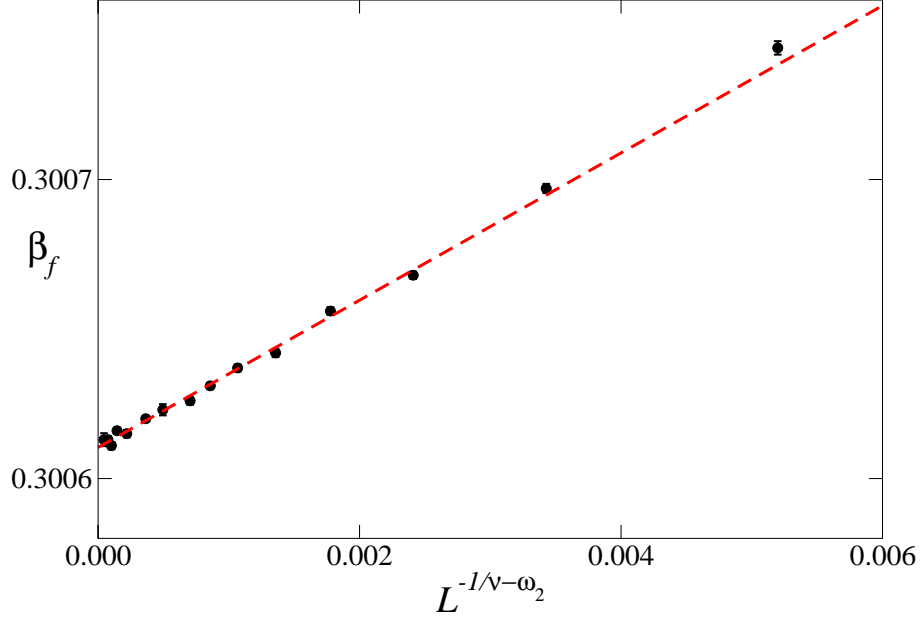


FIG. 11: Estimates of $\beta_f(L)$ at $p = 0.883$ versus $L^{-(1/\nu + \omega_2)}$ for $1/\nu + \omega_2 \approx 2.28$. The dashed line corresponds to a linear fit of the data for $L \geq 12$.

where $t \equiv T/T_{\text{Is}} - 1$, T_{Is} is the critical temperature of the Ising model, and k is a constant. No such mixing between t and w occurs in u_w , since u_w vanishes for $w = 0$. Hence, we can take $u_w = w$. The system has a critical transition for $w > 0$ at $T_c(w)$. Since the singular part of the free energy close to a critical point behaves as $(T - T_c)^{2-\alpha}$ ($\alpha = -0.049(6)$ is the specific-heat exponent of the RDIs universality class), we must have $F(X_c) = 0$, where X_c is the value of X obtained by setting $T = T_c(w)$ (see, e.g., Ref. 36 and references therein). Hence, we obtain

$$w [T_c(w)/T_{\text{Is}} - 1 + kw]^{-\phi} = X_c, \quad (24)$$

and therefore

$$T_c(w)/T_{\text{Is}} - 1 = (w/X_c)^{1/\phi} - kw + \dots, \quad (25)$$

where the dots indicate higher-order terms. This expression provides the w dependence of the critical temperature for w small. Note that the nonanalytic term in Eq. (25) is suppressed with respect to the analytic ones, because $1/\phi \approx 9.1$. Thus, $T_c(w) \approx T_{\text{Is}}(1 - kw + O(w^2))$. Since $T_c(w) < T_{\text{Is}}$, we can also infer that $k > 0$. From the results for $T_c(w)$ we estimate $k \approx 2.2$ for the $\pm J$ Ising model.

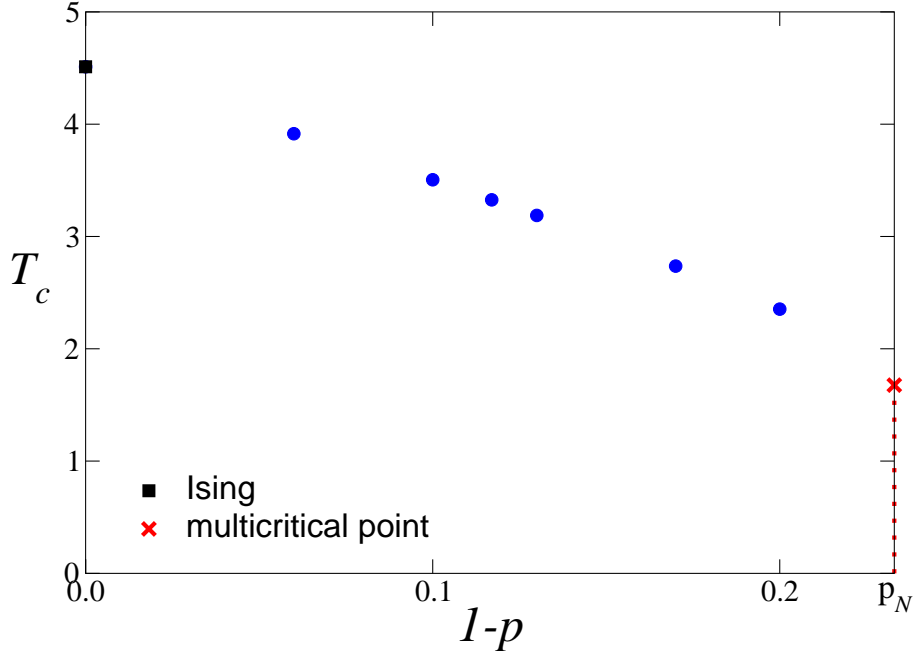


FIG. 12: The critical temperature $T_c \equiv 1/\beta_c$ vs $1 - p$.

V. CONCLUSIONS

In this paper we have studied the critical behavior of the 3D $\pm J$ Ising model at the transition line between the paramagnetic and the ferromagnetic phase, which extends from $p = 1$ to a multicritical (Nishimori) point at $p = p_N \approx 0.767$. We presented a FSS analysis of MC simulations at various values of p in the region $p_N < p < 1$. The results for the critical exponents and other universal quantities are consistent with those of the RDIs universality class. For example, we obtained $\nu = 0.682(3)$ and $\eta = 0.036(2)$, which are in good agreement with the presently most accurate estimates¹³ $\nu = 0.683(2)$ and $\eta = 0.036(1)$ for the 3D RDIs universality class. Therefore, our FSS analysis provides a strong evidence that the critical behavior of the 3D $\pm J$ Ising along the ferromagnetic line belongs to the 3D RDIs universality class.

We also note that the random-exchange interaction in the $\pm J$ Ising model gives rise to frustration, while the RDIs universality class describes transitions in generic diluted Ising systems with ferromagnetic exchange interactions. This implies that frustration is irrelevant at the ferromagnetic transition line of the 3D $\pm J$ Ising model. Moreover, the observed scaling corrections are consistent with the RDIs leading and next-to-leading scaling

correction exponents $\omega = 0.33(3)$ and $\omega_2 = 0.82(8)$. This indicates that frustration does not introduce new irrelevant perturbations at the RDIs fixed point with RG dimension $y_f \gtrsim -1$.

APPENDIX A: NOTATIONS

We define the two-point correlation function

$$G(x) \equiv \overline{\langle \sigma_0 \sigma_x \rangle}, \quad (\text{A1})$$

where the overline indicates the quenched average over the J_{xy} probability distribution. Then, we define the corresponding susceptibility $\chi \equiv \sum_x G(x)$ and the correlation length ξ

$$\xi^2 \equiv \frac{\tilde{G}(0) - \tilde{G}(q_{\min})}{\hat{q}_{\min}^2 \tilde{G}(q_{\min})}, \quad (\text{A2})$$

where $q_{\min} \equiv (2\pi/L, 0, 0)$, $\hat{q} \equiv 2 \sin q/2$, and $\tilde{G}(q)$ is the Fourier transform of $G(x)$. We also consider quantities that are invariant under RG transformations in the critical limit. Beside the ratio

$$R_\xi \equiv \xi/L, \quad (\text{A3})$$

we consider the quartic cumulants U_4 , U_{22} and U_d defined by

$$\begin{aligned} U_4 &\equiv \frac{\overline{\mu_4}}{\mu_2^2}, \\ U_{22} &\equiv \frac{\overline{\mu_2^2} - \overline{\mu_2}^2}{\overline{\mu_2}^2}, \\ U_d &\equiv U_4 - U_{22}, \end{aligned} \quad (\text{A4})$$

where

$$\mu_k \equiv \langle (\sum_x \sigma_x)^k \rangle. \quad (\text{A5})$$

We also define corresponding quantities \bar{U}_4 , \bar{U}_{22} , and \bar{U}_d at fixed $R_\xi = 0.5943$. Finally, we consider the derivative R'_ξ of R_ξ , and U'_4 of U_4 , with respect to $\beta \equiv 1/T$, which allow one to determine the critical exponent ν .

¹ H. Nishimori, Prog. Theor. Phys. **66**, 1169 (1981).

- ² P. Le Doussal and A.B. Harris, Phys. Rev. Lett. **61**, 625 (1988).
- ³ N. Kawashima and H. Rieger, in *Frustrated Spin Systems*, edited by H.T. Diep (World Scientific, Singapore, 2004); cond-mat/0312432.
- ⁴ H. Katzgraber, M. Körner, and A.P. Young, Phys. Rev. B **73**, 224432 (2006).
- ⁵ Y. Ozeki and H. Nishimori, J. Phys. Soc. Japan **56**, 3265 (1987).
- ⁶ R.R.P. Singh, Phys. Rev. Lett. **67**, 899 (1991).
- ⁷ Y. Ozeki and N. Ito, J. Phys. A **31**, 5451 (1998).
- ⁸ Refs. 5,6,7 report the estimates $p_N = 0.767(2)$, $p_N = 0.7656(20)$, and $p_N = 0.7673(3)$ respectively.
- ⁹ K. Hukushima, J. Phys. Soc. Japan **69**, 631 (2000).
- ¹⁰ A. Pelissetto and E. Vicari, Phys. Rept. **368**, 549 (2002).
- ¹¹ R. Folk, Yu. Holovatch, and T. Yavors'kii, Uspekhi Fiz. Nauk **173**, 175 (2003) [Phys. Usp. **46**, 175 (2003)].
- ¹² H. G. Ballesteros, L. A. Fernández, V. Martín-Mayor, A. Muñoz Sudupe, G. Parisi, and J. J. Ruiz-Lorenzo, J. Phys. A **32**, 1 (1999).
- ¹³ M. Hasenbusch, F. Parisen Toldin, A. Pelissetto, and E. Vicari, J. Stat. Mech.: Theory Exp. P02016 (2007).
- ¹⁴ P. Calabrese, V. Martín-Mayor, A. Pelissetto, and E. Vicari, Phys. Rev. E **68**, 036136 (2003).
- ¹⁵ A. Pelissetto and E. Vicari, Phys. Rev. B **62**, 6393 (2000).
- ¹⁶ H.G. Ballesteros, L.A. Fernández, V. Martín-Mayor, A. Muñoz Sudupe, G. Parisi, and J.J. Ruiz-Lorenzo, Phys. Rev. B **58**, 2740 (1998).
- ¹⁷ M. Campostrini, A. Pelissetto, P. Rossi, and E. Vicari, Phys. Rev. E **65**, 066127 (2002).
- ¹⁸ Y. Deng and H.W.J. Blöte, Phys. Rev. E **68**, 036125 (2003).
- ¹⁹ W. Janke, in Proceedings of the XXIII International Symposium on Lattice Field Theory, Dublin, July 2005, POS(LAT2005)018
- ²⁰ N. Ito, Y. Ozeki, and H. Kitatani, J. Phys. Soc. Jpn. **68**, 803 (1999).
- ²¹ P. Calabrese, P. Parruccini, A. Pelissetto, and E. Vicari, Phys. Rev. E **69**, 036120 (2004).
- ²² M. Hasenbusch, J. Phys. A **32**, 4851 (1999).
- ²³ M. Campostrini, M. Hasenbusch, A. Pelissetto, and E. Vicari, Phys. Rev. B **74**, 144506 (2006); Phys. Rev. B **63**, 214503 (2001).
- ²⁴ See, e.g., S. Wansleben, J.B. Zabolitzky, and C. Kalle, J. Stat. Phys. **37**, 271 (1984); G. Bhanot,

- D. Duke, and R. Salvador, Phys. Rev. B **33**, 7841 (1986).
- ²⁵ M. Lüscher, Comput. Phys. Commun. **79**, 100 (1994).
- ²⁶ The SIMD-oriented fast Marsenne twister random number generator has been introduced by M. Matsumoto and M. Saito. Details can be found in M. Saito, Master Thesis (2007) and at <http://www.math.sci.hiroshima-u.ac.jp/~m-mat/MT/emt.html>.
- ²⁷ In order to make the use of these expensive (in terms of CPU-time) generators affordable, we employed the same sequence of random numbers for the update of all n_{bit} systems (for the initialization of the configurations at the beginning of the simulation we used independent random numbers for each of the systems). This may give rise to a statistical correlation among the n_{bit} systems. This effect is probably small and we have not detected it. Anyway, in order to ensure a correct estimate of the statistical error, all n_{bit} systems that use the same sequence of random numbers have been put in the same bin in our jackknife analysis.
- ²⁸ R.H. Swendsen and J-S. Wang, Phys. Rev. Lett. **58**, 86 (1987).
- ²⁹ U. Wolff, Phys. Rev. Lett. **62**, 361 (1989).
- ³⁰ D. Ivaneyko, J. Ilnytskyi, B. Berche, and Yu. Holovatch, Physica A **370**, 163 (2006).
- ³¹ H.G. Ballesteros, L.A. Fernández, V. Martín-Mayor, A. Muñoz Sudupe, G. Parisi, and J.J. Ruiz-Lorenzo, Nucl. Phys. B **512**, 681 (1998).
- ³² The crossover exponent from pure Ising to RDIs critical behavior is the Ising specific-heat exponent³⁴ α_{Is} , see also Sec. IV C. This implies that the crossover scaling variable in the FSS at T_c is given by the combination $X = cwL^{\alpha_{\text{Is}}/\nu_{\text{Is}}}$, where $w = 1 - p$, $\alpha_{\text{Is}}/\nu_{\text{Is}} = 0.1740(8)$, and c is a normalization constant. When $w \rightarrow 0$, strong crossover effects are expected for $X \lesssim 1$, which corresponds to $L \lesssim (cw)^{-5.75}$. The RDIs asymptotic critical behavior is observed for $X \gg 1$.
- ³³ A. B. Harris, J. Phys. C **7**, 1671 (1974).
- ³⁴ A. Aharony, in *Phase Transitions and Critical Phenomena*, edited by C. Domb and J. Lebowitz (Academic Press, New York, 1976), Vol. 6, p. 357.
- ³⁵ I.D. Lawrie and S. Sarbach, in *Phase Transitions and Critical Phenomena*, Vol. 9, edited by C. Domb and J. Lebowitz (Academic, London, 1984).
- ³⁶ A. Pelissetto and E. Vicari, cond-mat/0702273.